Investigations of Fuel Cladding Chemical Interaction in Irradiated
LMFBR Type Oxide Fuel Pins by W.E. Roake, R.F. Hilbert, M.G. Adamson,
S. Langer, contributed by J.W. Weber, R.L. Gibby, E.T. Weber,
R.E. Woodley, the United States.

1.0 INTRODUCTION

Understanding and controlling the chemical attack of fuel pin
cladding by fuel and fission products are major objectives of the U.S.
LMFBR Mixed Oxide Irradiation Testing Program. Fuel-cladding chemical
interaction (FCCI) has been recognized as an important factor in the
ability to achieve goal peak burnups of 8 at% (80. MWd/kgM) in FFTF and
in excess of 10 at% (100. MWd/kgM) in the LMFBR demonstration reactors
while maintaining coolant bulk outlet temperatures up to ~600°C
(1100°F).

In this paper we review pertinent parts of the irradiation program
and describe recent observation of FCCI in the fuel pins of this program.
One goal of the FCCI investigations is to obtain a sufficiently quantita-
tive understanding of FCCI such that correlations can be developed
relating loss of effective cladding thickness to irradiation and fuel
pin fabrication parameters. Wastage correlations being developed using
different approaches are discussed.

Much of the early data on FCCI obtained in the U.S. Mixed Oxide
Fuel Program came from capsule tests irradiated in both fast and thermal
flux facilities. The fast flux irradiated encapsulated fuel pins con-
tinue to provide valuable data and insight into FCCI. Currently, however,
bare pins with prototypic fuels and cladding irradiated in the fast flux
Experimental Breeder Reactor-II (EBR-II) as multiple pin assemblies
under prototypic powers, temperatures and thermal gradients are providing
growing quantities of data on FCCI characteristics and cladding thickness

losses from FCCI. A few special encapsulated fuel pin tests are being
conducted in the General Electric Test Reactor (GETR) and EBR-II, but
these are aimed at providing specific information under irradiation
conditions not achievable in the fast flux bare pin assemblies or because
EBR-II Operation or Safety requirements dictate that the pins be en-
capsulated.

The discussion in this paper is limited to fast flux irradiation
test results from encapsulated pins and multiple pin subassemblies in
EBR-II and selected encapsulated tests irradiated in GETR. Other com-
parative tests in thermal reactors indicate that fast flux and thermal
flux results are similar.

An adequate understanding of FCCI requires integration of in-
reactor tests and out-of-reactor applied and fundamental studies. To
this end a Fuel Cladding Chemical Interaction Program has been estab-
lished involving several ERDA laboratories and contractors. Other
papers to be presented at this international meeting[1, 2, 3] will
describe; 1) FCCI work being carried on out-of-reactor but simulating
reactor irradiation conditions, 2) studies using all available data
sources aimed at illuminating the mechanism and developing models for
FCCI, 3) in-reactor and out-of-reactor tests using various techniques
and materials whose objectives are to prevent serious FCCI or to mitigate
its effect on fuel pin behavior, and 4) the application of FCCI data to
lifetime estimates and design criteria.

2.0 REVIEW OF IRRADIATION TESTS

Irradiation experiments have been conducted by Argonne National
Laboratory[4,5], General Atomics[6], General Electric[7], Oak Ridge
National Laboratory,[8] Westinghouse Advanced Reactor Division[9] and
Westinghouse Hanford[10,11] to obtain mixed oxide fuel pin performance
data. Tests which have emphasized investigation of FCCI are listed in
Table I, along with significant variables. This list includes only the
more recent experiments, and is current to the end of 1976.

All of these tests were designed to operate with peak cladding
temperatures at or above 600°C (1112°F) where significant cladding
attack occurs. To achieve these temperatures a fuel pin power of approxi-
mately 39.5 W/mm (12 kW/ft) is required. Several of the tests, particu-
larly the multiple pin tests, have included burnup as a variable by
conducting interim examinations wherein individual pins have been removed

and examined and replacements added to the subassembly for its continued irradiation. This approach, used extensively in the P-23 test series of subassemblies, has provided valuable metallographic data on the character and depth of FCCI as a function of burnup while holding other variables constant.

Type 316 cladding with 20% cold work has been the principal cladding studied as it is the current LMFBR reference cladding in the U.S.A. Other stainless steel cladding such as 304, 321, 347 and Ti modified 316 and other metallurgical states such as annealed and carbide agglomerated have also been included as in the GE F-11A and the HEDL P-23C tests to obtain data over a broader base. The principal variable in the fuel has been the initial O/M, ranging from 1.94 to 2.00 which covers the range of O/M for the reference fuel for Fast Flux Test Facility (FFTF) and Clinch River Breeder Reactor (CRBR). Plutonium oxide content was increased to 30 and 40% in the ANL-08 experiment, compared to 25% in the other tests. The object was to increase the ratio of Pu to U fissions to more nearly simulate the predominant Pu fission occurring in the non enriched LMFBR fuel. All of the bare pin subassemblies in Table I (F-11A, P-23A, P-23B and P-23C) are now under continuing irradiation in the run-to-cladding-breach phase of the program.

The P-23 Special Pins irradiated in the P-23B and P-23C subassemblies are intended to provide information on several gettering and buffering materials and on methods of placement for controlling or reducing the tendency for FCCI.[3]

The G. E. CAI and HEDL-GETR/RCT capsule tests in the GETR thermal reactor are designed to further investigate and verify mechanisms and understanding of cladding attack that are developed from out-of-reactor experiments.

3.0 U.S. FAST FLUX IRRADIATION EXPERIENCE

Results and analyses of past U.S. Fast Reactor irradiation experience with FCCI have been reported in various technical society conferences,[12,13] topical reports,[14] and periodic reports.[9,15,16] To develop a systemmatic review of the recent U.S. irradiation experience we discuss these results in three ranges of burnup; low burnup, (below 1.5 at%), intermediate (1.5 to 4.0 at%), and high (greater than 4.0 at%). The results are discussed in terms of the qualitative characteristics of FCCI and the observed effects of various fuel and irradiation parameters on FCCI.

From the metallographic examination of pins irradiated to various burnup levels, specifically the P-23A series, it is possible to observe the evolving character of the attack as a function of temperature along the length of the pin. The character of the cladding is classified by four types, namely: 1) matrix, 2) intergranular, 3) combined matrix and intergranular, and 4) deep localized attack. Figures 1 and 2 show typical photomicrographs of matrix and intergranular type of attack. The reaction product of the matrix attack, Figure 1, is a mixture of metal particles and nonmetallic compounds in the fuel-to-cladding gap. The attack on the grains is uniform with no strong preference for attack along the grain boundaries. In the intergranular attack, Figure 2, metallic and nonmetallic reaction products are also visible in the fuel-to-cladding gap and the grains have been chemically attacked, as evidenced by the roughened surface. In addition, however, this photograph shows opening of the grain boundaries from the cladding inner surface, indicating that attack has occurred along the grain boundaries.

3.1 Low Burnup - Less Than 1.5 at%

It has been shown both by calculation and by measurements on irradiated fuel pins that with slightly hypostoichiometric fuel such as in those pins in Table I, radial redistribution of oxygen occurs early in life. The oxygen migration down the temperature gradient provides an oxygen activity at the cladding surface sufficient to oxidize the chromium in the cladding. However, based on laboratory studies, significant cladding corrosion is not expected until fission products Cs and Te are available to participate in an enhanced corrosion process. The quantities required are small however, and sufficient quantities are generated by approximately 0.4 at% burnup to initiate the reactions. Thus, it is expected that even at burnups as low as 1 at% significant reaction can be observed. The reaction products typically observed in the P-23A fuel pin (1.2 at%) at peak cladding temperatures between 575 and 675°C (1067 and 1247°F) and at greater than 690°C (1274°F) are shown in Figures 1 and 2 respectively. Below 500°C (932°F) there was no cladding reaction, consistent with most reported data. From the temperature of the onset of cladding attack, approximately 525°C (977°F) to 675°C (1247°F) the character of attack was primarily matrix, Figure 1. Above 675°C (1067°F) the reaction character was mainly intergranular, Figure 2. The deepest intergranular penetrations of the cladding were 35 μm (0.0014 inch) in one or two localized regions.

3.2 Intermediate Burnup - 1.5 at% to 4.0 at%

Figure 3 shows the typical FCCI in a P-23A fuel pin at 2.4 at% burnup at temperatures up to 675°C (1247°F). As in the low burnup range, the reaction is principally matrix as shown in the optical micrograph. Electron microprobe examination revealed that the metallic reaction product is composed of Fe and Ni. Cr and Cs appear adjacent to the cladding in a nonmetallic form, probably oxides. Te is occassionally found along with the Cs and Cr. Mn and Mo frequently form nonmetallic layers of high concentration, usually between the Cr + Cs layer and the metallic Fe + Ni reaction product layer. As at the lower burnup range the threshold temperature for attack was approximately 525°C (970°F) with the depth of attack and thickness of reaction product increasing with temperature.

Above 675°C (1247°F) the character changes as at the lower burnup from matrix to intergranular, Figure 4. The intergranular attack is extensive with some areas of attack as much as 25 μm (0.001 inch) deep. Whole grains on the cladding edge are surrounded by intergranular attack and the carbides have begun to disappear from the grains as well as from the grain boundaries. These observations show similarity with the character found at the lower burnup in this temperature range. However, the frequency of its occurrence is much greater. Electron microprobe examination shows that Cr is depleted at grain boundaries from which carbides have disappeared.

Results from fuel rod G-3 of the Gulf Atomic (GA) F-1 experiment irradiated to 2.7 at% at a maximum cladding temperature of 695°C (1283°F) showed less depth of cladding attack, approximately 8 μm (0.0003 inch), than the comparably irradiated P-23A pin. The O/M in G-3 was about the same as P-23A, 1.987. The fuel in G-3 was derived from Sol Gel.

Results from the P-23B fuel pins at approximately 2.3 at% burnup, are significantly different from those of P-23A in terms of the character of cladding attack above 675°C (1247°F). Figures 5 and 6 show typical photomicrographs of the fuel cladding interface in pins P-23B-49C and -62D, respectively. A loose metallic and nonmetallic matrix reaction product fills the gap in pin P-23B-49C. In pin P-23B-62D a dense matrix reaction type of attack is visible on the cladding surface approximately 3 μm (0.0001 inch) thick. In neither of these P-23B pin is there evidence of any of the intergranular cladding attack observed in the P-23A pin at this burnup where temperatures were above 675°C (1247°F), (Figure 4). There is also no indi-

cation of carbide disappearance along grain boundaries of the P-23B pin cladding as was observed in P-23A. The difference in type of attack between the P-23A and P-23B pins and the lesser matrix attack in pin P-23B-62D than in P-23B-49C is attributed to a difference in the fuel initial O/M and the consequent effect on oxygen activity. The O/M in P-23A irradiated to 2.4 at% was 1.984 whereas P-23B-49C was 1.97 and P-23B-62D was 1.95.

3.3 High Burnup - Greater Than 4 at%

In a P-23A pin irradiated to 5.0 at%, the predominant attack up to approximately 680°C (1256°F) is matrix type as found at the lower burnup. However, in contrast to the intergranular attack predominant above 675°C (1247°F) at the lower burnup, the character at 5.0 at% has changed to a matrix attack shown in Figure 7. This form of matrix reaction we refer to as advanced or evolved matrix attack. Evidence of the change in reaction character can be seen in photomicrographs of some areas on the fuel pin at 2.4 at% burnup in the temperature range above 680°C (1256°F).

At this higher burnup, greater than 4 at%, whole grains have been lost or detached from the cladding. In other grains still attached to the cladding, the carbides have completely disappeared. Electron microprobe results, Figures 8 and 9, reveal that the grains and grain boundaries where carbides have disappeared are depleted in Cr, leaving Fe + Ni enhanced areas similar to, but more extensive than observed at lesser burnups. The Cs and Cr are present in the same general area in a nonmetallic form, probably an oxide, next to the cladding, Figure 10, where they appear localized in high concentrations adjacent to the chromium depleted grains. Layers of Mn and Mo are found in the gap between the Fe and Ni reaction product and the Cs + Cr layer. Fission products are found in the attacked grain boundaries but not in the grains or grain boundaries where carbides have disappeared.

Fuel pin G-6 of the GA F-1 irradiation experiment also showed progression of cladding attack from intergranular to matrix. This fuel pin with an original fuel O/M of 1.972 was irradiated to 5.4 at% at a peak cladding temperature of 685°C (1265°F). The maximum measured depth of cladding attack was 25 μm (0.001 inch). Metallographic examination of pin G-1 irradiated to 5.6 at% burnup at 760°C (1400°F) peak cladding temperature revealed deep attack, 66 μm (0.0026 inch). The attack occurred between radial fuel cracks and is not as deep at the ends of the fuel cracks. This is consistent with the HEDL observations that

greater attack tends to occur where the fuel and cladding are in close contact, rather than at the open end of the radial fuel cracks.

Early metallographic examination of P-23A pins irradiated to approximately 10 at% shows that the character of the reaction continues to evolve toward matrix at temperatures above 675°C (1247°F).

As at 2.3 at% the metallography performed on the lower O/M P-23B pins at 5.3 at% shows a continued matrix reaction, the depth of which is dependent on the initial fuel O/M. The matrix reaction product on P-23B-2A after irradiation to 5.3 at% at greater than 675°C (1247°F), Figure 11, is metallic, dense and of relatively uniform thickness, about 13 μm (0.0005 inch). There is some indication of a preferred attack at grain boundaries, but much less than the intergranular attack in P-23A at 2.4 at%. The matrix reaction on P-23B- 40B with an O/M of 1.95 is also metallic and dense, Figure 12. By comparison, however, the reaction product layer is only one fourth to one third as thick as in P-23B-2A with the O/M of 1.97, indicating less cladding attack in the pin with lower O/M. Cladding on P-23B pins, -2A and -40B show the disappearance of carbide particles in the cladding grain boundaries at 5.3 at%, similar the observations on P-23A pins at 2.4 at% burnup. At 2.3 at% the P-23B pins showed no disappearance of carbides. The depth into the cladding to which the carbides disappear is approximately the same on the twc P-23B pins, suggesting that at this burnup the difference in O/M levels did not significantly affect this phenomenon.

Two fuel pins in the GE F-10B experiments also demonstrated the effect of lower fuel O/M in reducing penetration of the cladding. Fabrication parameters and fuel-cladding chemical interaction data from Rods F10B-21 and F10B-25, which focused on the effect of fuel stoichiometry, are given in Table II. Note that compared to Rod F10B-21 (O:M = 1.97), Rod F10B-25 (O:M = 2.00) exhibited a deeper maximum penetration, 96 μm (3.8 mils) versus 56 μm (2.2 mils) and a larger amount of affected circumference (96% versus 40%) at the highest temperature region even though cladding temperature, power, and burnup were slightly less. Data from the F10B fuel pins which demonstrate the O:M dependence of chemical interaction between mixed-oxide fuel and 20% cold-worked Type-316 SS are consistent with thermal flux test results on Type-304 SS cladding[17] and fast flux data obtained at ANL on solution-annealed Type-316L SS cladding[18] as shown in Figure 13.

The change in character of attack above 675°C in the higher O/M P-23A pins from intergranular at lower burnup to matrix or evolved matrix at burnup between 2.0 and 5.0 at% appears consistent with a mechanism involving oxidation of the cladding constituents. It has been proposed that early in the irradiation ($\leq$ 1 at%) of hypostoichiometric fuels (O/M $\approx$ 1.98), the protective oxide film of Cr_2O_3 is disrupted by the chemical action of Cs and Te fission products. The exposed cladding grain boundaries are then attacked, exposing greater surface to the oxygen and fission products. Eventually whole grains become surrounded and loosened from the cladding, as observed at 2.4 at%. Chromium is apparently preferentially oxidized as the electron microprobe shows Cr depletion in grain boundaries in advance of the attack, adjacent to already reacted grain boundaries at 2.5 at% and in whole grains at 5.0 at%. The increased surface area available for oxidation and reaction by fission products may account for the predominance of matrix over grain boundary attack at high burnup. It is considered more likely, however that more complex changes in mechanism occur as a result of changing concentrations of Cr and carbon, longer diffusion paths and most importantly because the oxygen activity gradually increases in the fuel pin as a result of fission. Details on Laboratory studies[1] and mechanisms[2] developed to explain these observations are presented in companion papers at this conference.

4.0 U.S. THERMAL REACTOR AND OTHER SPECIAL TESTS

Experiments are being conducted in GETR to obtain specific information for FCCI that require capsule designs, instrumentation and or controls for which that reactor is better suited than the EBR-II.

4.1 CAI Test Series

The CAI (Cladding Attack Inhibition) Test series is designed to study the effectiveness of various cladding attack inhibitors under typical irradiation conditions.[19,20] Characteristic radial and axial temperature gradients are produced inside four miniature (doped) fuel pins by irradiating them inside an instrumented capsule in the General Electric Test Reactor (GETR). The principal objectives of the CAI test series are: (a) to demonstrate induced intergranular attack (IGA) by responsible fission products (Cs, Te) in an irradiated fuel pin, (b) to demonstrate the effectiveness of Nb buffer as an inhibitor of cladding IGA, and (c) to establish the essential conditions inside a fuel pin for occurrence of deep fission product (Cs, Te)-induced intergranular penetration of Type-316 stainless steel cladding.

4.1.1 Description

In the CAI series four 100 mm (4 inch) long fuel pins are joined end to end in the capsule which is instrumented to measure temperatures at two axial locations. The capsules are irradiated in the GETR V-RAFT facility. Cladding temperatures are maintained in a temperature range sufficient to promote FCCI, 600 to 750°C (1112°F to 1382°F).

The fission product additives were placed in cavities in the central fuel pellets. In the CAI-1 test the Cs, Te fission products were added separately as Cs_2CO_3 + 3/2 Nb (source of Cs and C), and as elemental Te. In CAI-2 they were incorporated as cesium telluride, Cs_2Te. The mixed oxide pellets were enriched with U-235 (25 wt% PuO_2 - 75 wt% UO_2, 65% U-235) to achieve the desired cladding temperatures, and O:M ratios were varied in the range 1.96-1.99. Certified Type-316 stainless steel tubing and rod, 20% cold-worked, were used to fabricate the fuel pin hardware. The cladding thickness was nominally .38 mm (.015 inch).

The matrix for the CAI-1 and -2 tests is shown in Table III. In each test two pins untreated were used as controls and two pins incorporated niobium, in two different locations as the buffer/getter material. Thin coatings of Nb were applied (by sputtering) to the outer surfaces of fuel pellets for pins CAI-1-I (12 μm, .0005 inch thick) and CAI-2-VIII (25.4 μm, .001 inch thick). In pin CAI-1-II twisted Nb wires were inserted into the upper and lower section of the central hole of the annular fuel pellet column. In each pin sufficient Nb was added for effective inhibition of FCCI (150-450 mg per 15 gm fuel). Based on the estimated yield of tellurium fission products the quantities of added Cs, Te in the two sets of fuel pins corresponds to ∿ 50 at% burnup (CAI-1) and 2-6 at% burnup (CAI-2). On the basis of out-of-pile FCCI test results the conditions inside the fuel pins during irradiation (i.e. cladding inner surface temperature, fuel O:M at the outer surface, Cs:Te ratio) were chosen to produce observable intergranular attack of the cladding inner surface 102-127 μm (0.004 - 0.005 inch) in the absence of an inhibitor such as Nb.

CAI-1 was irradiated in three steps; 120 hours at cladding temperature of 340°C (644°F), 128 hours at 595 to 645°C (1103 to 1193°F) cladding temperature, 128 hours at 630 to 705°C (1166 to 1300°F). The fuel pins failed near the end of the second step, revealed by later examination.

4.1.2 Observations and Results

Typical photomacrographs, Figure 14, show severe attack in the inner surface of the cladding had taken place in each of the miniature pins. From high magnification photomicrographs it is apparent the cladding was attacked simultaneously by a dissolution process, and intergranular attack, Figure 15. Bright metallic particles throughout the fuel matrix were typically observed at axial locations where the cladding was heavily attacked. In some locations typically at fuel pellet interfaces - metallic "rivers" appeared to flow from the cladding inner surface almost to the center of the fuel. Estuarine configurations at the river-cladding intersections suggest that attack was most rapid at these locations.

Transverse sections from CAI-1-I and CAI-1-II fuel pins, Figure 16, show metallic-appearing inclusions distributed throughout the fuel (including "rivers"), a NaK-fuel reaction phase at the fuel periphery (Na and K both detected in this phase), and (in CAI-1-I), apparent absence of the original 12 μm (.005 inch) thick Nb coating on the fuel pellets.

Microprobe measurements revealed that Fe, Cr and Ni from the cladding became distributed as metallic particles throughout the fuel in both fuel pins. In sample CAI-1-I intensity ratio measurements on these particles and in the unreacted cladding showed iron to have been preferentially transported towards the center of the fuel, and transport of nickel to be slightly greater than of chromium. Niobium also appears to undergo preferential transport towards the fuel center where it tends to associate with iron in the metallic particles. Although Cs and Te were both present at the fuel-cladding interface, neither could be detected in the metallic particles within the fuel.

4.1.3 Conclusions

The cladding dissolution and mass transport process which occurred in the CAI-1 fuel pins tended to mask any inhibition of cladding IGA that might have resulted from the presence of Nb buffers in two of the pins (I and II). It is to be noted, however, that more intergranular penetration was observed in the two pins that did not contain Nb 127 μm to 203 μm (.005 to .008 inch) than in pins I and II 50 to 76 μm (.002 to .003 inch). However, because the cladding was completely penetrated in all four pins at other locations, this observation cannot be accepted as evidence for an inhibitory effect. The CAI-1 test results and other

pertinent data are summarized in Figure 17. GE out-of-reactor test data also have been plotted to indicate the amount of IGA expected in the CAI-1 test in the absence of thermal transport effects. There is fair agreement between the observed intergranular penetration in the nonbuffered CAI-1 rods and the out-of-reactor Cs, Te-induced attack data. The obvious discrepancies between the total cladding wastage in the GETR capsule tests and the out-of-reactor predictions give a measure of the contribution of mass transport to total cladding inner surface wastage in a reactor environment. The proposed cladding dissolution-mass transport process appears to require relatively large quantities of (liquid) Cs and Te and a steep radial temperature gradient. It is hypothesized that a liquid metal phase (Cs, Te) is necessary to dissolve and transport the cladding components and that the observed redistribution of Fe, Cr, and Ni in the temperature gradient is determined by the relative solubilities and thermodynamic stabilities (ΔH°) of their respective tellurides. Current CAI results provide no evidence that the mass transport process depends on the oxygen activity of the fuel. However, additional information on this point is being developed through out-of-reactor experiments.[1]

4.2 GETR Reirradiation Test (RCT)

The GETR Reirradiation Test (RCT) designed to evaluate the effect of different fuel pin chemical conditions on fuel-cladding chemical interaction and fission product redistribution was conducted by HEDL using both fast (EBR-II) and thermal Reactor (GETR) irradiation conditions.[21] The primary objective of the tests was to determine the effect of oxygen chemical potential (controlled by varying ^{235}U enrichment and burnup) in a fuel pin during irradiation, on the chemical reactions and mass transport phenomena which impact fuel pin performance.

4.2.1 Description

Four* EBR-II experimental mixed-oxide fuel pins with different ^{235}U enrichments and burnup levels were selected for reirradiation in the GETR. In addition to the fuel pins selected for reirradiation, sibling pins from the EBR-II portion of the irradiation were selected for examination in comparing with the reirradiated pins to establish the conditions of the fuel pins prior to their reirradiation at increased operating temperatures. All fuel pins reirradiated in the GETR experienced nearly identical conditions of time and temperature. Thus, differences in their

---

*A fifth pin, which was identical in burnup and enrichment to one of these four, was also irradiated in GETR.

behavior during the reirradiation were a result of their as-fabricated enrichment differences plus the prior irradiation at different heat ratings and to different burnup levels.

The selected fuel pins had operated in the EBR-II at peak cladding temperatures less than necessary for measurable cladding oxidation, ~550°C (1022°F). Table IV summarizes the specific enrichment and operating parameters which were included in the experiment. To initiate corrosion, the pins were reirradiated for a specific period of time at increased cladding temperatures in the GETR. The cladding inner surface temperatures were increased in the GETR to approximately 700°C (1292°F) as monitored by thermocouple and controlled by GETR-RAFT variable positioning/power capability. Fuel temperatures calculated for the axial position corresponding to peak cladding temperature were typically 1900-2100°C (3452-3812°F) at the centerline and 800-1100°C (1472-2012°F) at the fuel surface. The irradiation at the increased temperature was continued 650 hours. This additional exposure was calculated to not significantly alter the overall chemical composition within the fuel pins established during the EBR-II irradiation. From a direct comparison of the extent of cladding attack and fission product distributions among the four fuel pins, the relative effects of the ^{235}U enrichment and burnup on chemical behavior could be assessed.

4.2.2 Observations and Results

Of the four major test matrix elements (combined burnup-enrichment levels) represented in the experiment, only three yielded significant information on chemical behavior. Two identical pins, representing the high burnup, natural urania conditions (see Table IV) suffered cladding breaches[22] which allowed the ingress of NaK, thereby adversely perturbing the fuel chemistry. Nevertheless, considerable information pertinent to understanding fuel-cladding chemical interaction and fission product redistribution was obtained.

Oxidizing conditions at the fuel surface were estimated by calculating the increase in the fuel O/M with burnup and the redistribution of oxygen toward the fuel surface as a consequence of the radial temperature gradient. Estimates of fuel surface O/M and ΔG_{O_2} for both the low cladding temperature EBR-II irradiation and the high cladding temperature GETR irradiation are summarized in Table V.

Cladding corrosion in the reirradiated fuel pins was generally consistent with thermochemical predictions. Oxygen potentials and fission-product concentrations sufficient for cladding attack were

generated during the EBR-II irradiation, but measurable attack did not occur because of the low cladding temperatures. Examination of the sibling pins revealed little or no evidence of cladding corrosion. Reirradiation conditions in the GETR provided the temperature necessary to overcome kinetic limitations to the reaction. The significant differences in FCCI in the reirradiated pins, as established by ceramographic and electron microprobe examination, are presented in Table VI. Only the highest burnup ($\sim$ 7.0 at%) pin sustained a significant depth of attack, typically intergranular, which appeared to have affected approximately 1/3 of the inner cladding surface in the top 1/3 of the fuel pin. Except for these regions of aggressive grain boundary corrosion in the higher burnup pin, the extent of generalized (matrix-type) corrosion in all three irradiated pins was similar. Since the time at temperature and the thermal condition in GETR were essentially the same, and since the fuel surface O/M (Table V) is calculated to be essentially equivalent for all three pins, occurrence of more severe attack in the one case is interpreted to reflect the impact of higher fission product concentrations, either through increased oxygen potential at the fuel surface or a difference in available fission products at the fuel-cladding interface. On the other hand, since the extent of matrix-type corrosion was similar in the three pins, it appears that matrix attack was controlled by the kinetics of the corrosion reaction (i.e. the time at temperature in the GETR) rather than by the rate at which excess oxygen and fission products were generated and/or transferred to the cladding surface.

Cesium, a principal fission product involved in cladding corrosion, can also react locally with fuel and UO_2 blanket/insulator pellets. Cesium distribution in the pins was mapped using radial and axial gamma scanning techniques and shielded electron microprobe examination. Although some cesium appeared to remain in the inner regions of the fuel, radial mapping indicated that thermal gradients were sufficient to move the bulk of the cesium to the cooler fuel circumference in all pins in the series. Axial relocation of cesium was principally toward the cooler, lower end of the fuel column. Substantial concentrations of Cs occurred in the fuel column rather than at the extreme ends, for both the higher and lower burnups. Differences among pins were apparently related to differences in the axial variation in fuel-cladding gap temperatures and fuel surface oxygen potentials.[23]

The relative locations of some other gamma-active fission products were determined and compared with the corresponding burnup profiles to establish if any significant redistribution occurred. Only ^{140}La exhibited relocation toward the cooler regions of the fuel, similar to the movement of cesium.

Enhancement of the Pu/U ratio in the outer, lower temperature regions of the fuel in the intermediate-power, moderate-burnup fuel pin (PNL-4-14) occurred during reirradiation, contrary to predictions. Neither of the corresponding low burnup pins nor any of the sibling pins exhibited significant plutonium relocation, consistent with expectations based on the lack of vapor-phase transport of plutonium at the peak fuel temperature involved in this experiment. Currently, there is no adequate explanation for the Pu enhancement near the fuel surface in the PNL-4-14 pin.

4.2.3 Conclusions Significant to LMFBR

The conclusions from the GETR reirradiation experiment results most significant to the understanding and prediction/modeling of fuel-cladding chemical interaction in LMFBR fuel pins are:

- Comparison of fuel surface oxygen potentials (calculated from radial O/M gradient models) to chromium oxidation thresholds yields consistant results in predicting the presence of cladding corrosion but does not provide a sufficient basis for indicating the (probable) occurrence of significant (intergranular) cladding attack in irradiated fuel pins.

- An O/M ratio as low as 1.96 at start of irradiation does not reduce oxygen chemical activity sufficiently to prevent reaction in all high burnup cases. The test demonstrated that reactant concentrations and chemical activities were sufficient at $\sim$ 7 at% burnup to cause significant intergranular attack.

- Local concentrations of some fission products appeared responsible for deep intergranular cladding attack. Conversley, the extent of matrix-type corrosion appeared less dependent on fission product concentration (burnup) and thus is concluded to be controlled by the kinetics of the corrosion reaction.

- Any increase in fuel pin cladding temperature into the 650-700°C (1202-1292°F) range following moderate burnup at lower temperature has the potential of producing significant intergranular corrosion in a few hundred hours.

5.0 WASTAGE CORRELATIONS

Characterizations of FCCI in the irradiated fuel pins as described in Section 3.0, plus results from out-of-reactor experiments have helped identify important variables of fuel and irradiation that affect FCCI. From this insight, models and correlations are being developed with which to predict and design for control of FCCI in fuel pins.

The principal concern of the fuel pin designer is how much cladding loss to allow for, for various combinations of fabrication and irradiation parameters. Although much data have been collected on FCCI, the range of variables and the uncertainty of some of the irradiation parameters (particularly temperature) presents serious obstacles to developing consistent correlations. Two approaches are followed in the U.S.A. One is to limit the data base to a few fuel pins with few fabrication and irradiation variables for which the irradiation conditions are well known, or definable by relation to a sibling pin with high confidence. The other approach is to include all the FCCI data, except for that completely unreliable, and work from a broader but lesser understood base of data.

Also there is not yet any in-reactor experimental evidence of how FCCI effects the mechanical behavior of the cladding. That is, is the cladding behavior affected more by the deepest intergranular attack or by an averaged depth of attack over some portion of the cladding circumference.

HEDL currently includes only data from the P-23 series pins in a correlation being developed to relate average depth of cladding attack to temperature, burnup and, ultimately, fuel O/M. G. E. is developing a similar correlation related to maximum depth of cladding attack that is incorporating data from a broader range of fuel pins. This correlation includes cladding irradiation temperature, duration of the irradiation, burnup, linear power, O/M, and smear density as variables.

5.1 HEDL Wastage Correlation

The current HEDL wastage correlation, incorporates data from three P-23A fuel pins. Revisions are in progress to include data from P-23A, P-23B and P-23C pins (Table I).

HEDL P-23A is an assembly of 37 pins irradiated in Mark J-37 sodium by-pass EBR-II hardware.[10,11,14] The fuel pins described in Figure 18 contain a 343 mm (13.5 inch) long column solid pellets of 25 w/o PuO_2-75 w/o UO_2. Each pellet is 3.3 mm (.21 inch) long by 4.9 mm (.19 inch) in diameter with dished ends fabricated by mechanical mixing, pressing and sintering. At start of irradiation the pellet density was 90.5% of theoretical and the nominal planar smeared density was 85.5% of theoretical.

Interim examinations produced data on FCCI at 1.2, 2.4, and 5.0 at% peak fuel burnups. The cladding inner surface temperatures ranged from 410°C at the sodium inlet end to 720°C (1328°F) at the top of the fuel column. The analysis described in this paper is based upon the results of destructive examination of one pin at each of the three exposure levels. In the lowest burnup pin the initial fuel O/M was 1.978. In the other two pins the initial fuel O/M was 1.985. The small difference in O/M was not considered to be significant at the time the correlation was developed. A refinement being incorporated into the revised correlation will include the O/M variable.

Each pin was sectioned for metallographic examinations at five or six positions along the length of the fuel column. Polished metallography samples prepared using non aqueous grinding and polishing lubricants, were visually examined and photographed at 350x and 750x at 8 or 16 equally spaced positions around the circumference of the fuel-cladding interface. The depth of cladding attack was measured on each photomicrograph.

Because the products of the matrix type reaction are sometimes loose in the fuel to cladding gap, some criterion is necessary for measuring the depth of attack. Figure 19 illustrates this measurement on cladding exhibiting matrix reaction. Sufficient areas of no attack exist adjacent to significant matrix reaction to establish a ratio of reaction layer thickness to cladding penetration that could be used to locate the plane of the original inner surface on other micrographs. Intergranular attack was measured from the estimated original inner surface to the point of deepest intergranular attack on each micrograph and averaged to obtain a single value for each cross section.

Penetration of the cladding on each section of the fuel pin represents the cumulative effect of time and varied temperature. Analysis of the time-temperature relationship for each pin using EBR-II postrun flow and fission rate data showed that variations during reactor full power operation were approximately ± 20C° (37F°). The cladding inner surface temperatures used in this analysis were calculated from fuel pin power based on the chemically measured fuel pin burnup, and the axial power variation determined from postirradiation $^{95}Zr/^{95}Nb$ gamma scanning of the fuel pins.

Table VII shows cladding penetration measurements for each pin. In all cases, except the lowest exposure pin, the maximum measured penetration is approximately twice the average.

Figure 20 shows the average penetration data plotted as a function of cladding inner surface temperature. Each point represents an unique place along the fuel pin and an unique time averaged temperature. The plots shows an increasing penetration with temperature starting from approximately 450 to 500°C (842 to 932°F) and an increasing penetration with burnup for a constant temperature. The form of the correlation equation was chosen to provide an exponential temperature relationship and a power dependence of burnup. Non-linear regression analysis of the data yields the following equation,

$$D = 2.43 \times 10^6 \, [B.U.]^{0.517} \, \exp[- \frac{9806}{T}]$$

where D is the averaged penetration of the cladding in μm, B.U. is the average fuel pin burnup in at% and T is the cladding inner surface temperature in °K. The burnup is to the one half power, or approximately to the square root of time, thus these data show a decreasing rate of penetration with time or burnup.

The curves of the equation for the three average burnups representing the plotted data are also shown in Figure 20. The curves and the data show reasonably good fit.

5.2 G. E. Wastage Correlations

To assure a safe and licensable LMFBR design, a viable correlation must be developed which takes into account as wide a sampling of data as possible. It is also clearly desirable that the accepted correlation be based on a sound chemical understanding of the cladding attack process. A correlation has been developed which gives the best fit to all the available data on maximum depth of cladding attack and, in addition, uses an analytical form of the correlation which was specified to be consistent with current knowledge of cladding attack mechanism.

It was found in preliminary statistical analyses that a data bank of 68 pin sections[24] can be correlated to a fair degree with the functional form

$$D = At^b e^{\frac{Q}{R \, T_c}} \, f(P)$$

where

D = maximum depth of cladding intergranular attack, μm
t = pin irradiation time, equivalent full power days
T_c = cladding inside surface temperature, °K
P = maximum (peak) linear power
R = gas constant, 1.987 cal/gmole °K
A,b,Q = correlation constants

In addition, it was observed that the standard error of correlations can be further reduced by including in the correlation other fabrication and operating parameters, such as pin oxygen activity and fuel smeared density. The linear powers and burnups used in the correlations are based on the EBR-II Experimenters Guide fission rate data. The cladding temperatures are those of the cladding inner surface at the start of life.

Of several correlations developed the following was chosen because of the simplified form and low standard error.

$$D = 2.36 \times 10^8 \, \exp \frac{-14185}{1.987T(°K)} \, t(0:M + 0.001 \, BU - 1.96)Q^{2.33}(1-p)$$

where D = maximum depth of cladding intergranular attack, μm, T = cladding inside surface temperature °K, t = equivalent full power days of irradiation, O/M = initial fuel oxygen to metal ratio, BU = atom % burnup, ρ = Smear density (fraction of theoretical). Q = Peak linear power (w/mm).

The form of the correlation was chosen to reflect current knowledge of probable cladding attack mechanisms. Since most thermally activated processes exhibit exponential temperature dependence, it is reasonable to assume the same to describe cladding attack. The initial temperature to be used is that of the cladding inner surface. An effective activation energy probably representing several thermally activated processes of 14.2 kcal/mole is in reasonable agreement with similarly defined quantities deduced from out-of-reactor studies, 15 to 30 kcal/mole.[17,18,25,26]

The time variable was originally treated as a power function since reasonable assumptions regarding mechanisms indicate a parabolic time dependence (cladding attack rate dependent upon diffusion of the reactants at cladding surface). The exponent was allowed to float during

the maximum likelihood calculation in order to determine a trend toward parabolic or linear dependence. In the correlation with the minimum standard error the exponent of time was 0.8. In the correlation chosen, the exponent was arbitrarily set at unity, giving a linear time dependence.

The stoichiometry term was formulated on the basis that cladding attack depends on oxygen potential. Out-of-reactor studies[25,27] have shown that no fission-product-induced cladding attack occurs so long as the oxygen potential at the fuel-cladding interface is below the oxidation threshold for chromium in the stainless steel, which corresponds to a fuel stoichiometry of approximately 1.996 at typical fuel-cladding interface temperatures. Since oxygen redistribution in the fuel will result in approximately a 1.996 oxygen-to-metal ratio at the fuel surface when the average O:M is about 1.96,[28] setting the fuel stoichiometry below this point would be expected, per se, to eliminate cladding attack. The increase in oxygen potential with burnup is accommodated by the term (0.001 B.U.) which is based on recent data indicating that oxygen release during fissioning amounts to 0.001 O/M units per at% BU. Intuitively, fission products and oxygen would be expected to be driven toward the fuel-cladding interface with greater efficiency as the fuel temperature gradient increases. Thus, increasing the (local) linear power should make more fission products and oxygen available to act upon the cladding. Therefore, a term in the correlation involving linear power is proper (peak linear power is used in the correlations to allow comparisons between fuel pins). The porosity should interact in a similar manner to the linear power in that an increase in porosity (decrease in smear density) would be expected to enhance transport of fission products and oxygen toward the fuel-cladding interface.

A plot of the cladding-penetration predicted by the G.E. correlation for two different sets of operating condtions is shown in Figure 21. A plot of the measured cladding attack data used in the GE correlation versus that calculated using the statistical correlation is shown in Figure 22 along with the uncertainty limits on the correlation (± 1σ).

5.3 Discussion on Correlations

The HEDL correlation predicts "average of maximum" depths of attack based on measurements of the maximum attack at several sampled locations around the inner surface of the cladding. The GE correlation predicts the maximum depth of attack based on the measurement of the deepest attack anywhere around the inner surface of the cladding. Thus these correlations each predict different aspects of the depths of attack. If the cladding load bearing capability under irradition is limited by the thinnest cross section at the end of the deepest grain boundary penetration then the GE correlation predicts that amount of cladding loss that must be considered in fuel pin design. If, however, the load bearing capability is more related to averaged properties over some significant part of the cladding circumference then the HEDL correlation predicts a lesser amount of cladding wastage. The real effects that FCCI have on load bearing capabilities have not been clearly defined and are the subject of another paper in this conference[3].

The basic objective of the HEDL correlation is to predict the depth of cladding attack for the FFTF/CRBR reference fuel pin with 316-20% cold worked cladding. The predicted and measured attacks for the P-23A fuel pins at 5.3 at% burnup are very close as shown in Table VIII. The GE correlation which is intended to cover a much broader range of the irradiation and fabrication parameters tends to overpredict the maximum depth of attack for the same P-23A fuel pins. As more data from fuel pins with reference cladding and fuel become available both correlations will be recalibrated, and adjusted to include the effects of O/M, temperature and burnup on cladding attack both as an average attack and as maximum attack depth.

REFERENCES

1. M. G. Adamson, "Out-of-Pile Experiments Performed in the U.S. Fuel Cladding Chemical Interaction (FCCI) Program," IAEA Specialists Meeting on Fuel Cladding Interactions, Tokyo, Japan February 21-25, 1977.

2. M. G. Adamson, "Mechanisms of Fuel Cladding Chemical Interaction: U.S. Interpretation," IAEA Specialists Meeting on Fuel Cladding Interaction, Tokyo, Japan, February 21-25, 1977.

3. R. J. Jackson et al, "Implications and Control of Fuel-Cladding Chemical Interaction for LMFBR Fuel Pin Design," IAEA Specialists Meeting on Fuel Cladding Interaction, Tokyo, Japan, February 21-25, 1977.

4. J. D. B. Lambert et al, "Performance of Mixed-Oxide Fuel Elements-ANL Experience," Proceeding of the Conference on Fast Reactor Fuel Element Technology, ANS, April 1971, p. 517.

5. L. A. Neimark, J. D. B. Lambert, W. E. Murphy, R. W. Renfro, "Performance of Mixed-Oxide Fuel Elements to 11 at% B.U." Nucl. Tech. 16 (1972) p. 75.

6. J. R. Lindgren et al, "Irradiation Testing in the Development of Fuel Elements for the Gas-Cooled Fast Breeder Reactor," Fuel and Fuel Elements for Fast Reactors, Vol 1, IAEA 1974, p. 111.

7. C. N. Craig et al, "Steady State Performance of PuO_2-UO_2 Fast Reactor Fuels," Proceeding of the Conference on Fast Reactor Fuel Element Technology, ANS, April 1971. p. 555.

8. Fast Breeder Reactor Oxide Fuels Department - Final Report - ORNL-4901, November 1973.

9. Oxide Fuel Element Development Quarterly Progress Report, WARD-OX Series Starting September 1968 and continuing.

10. HEDL Steady-State Irradiation Testing Program - Status Report, HEDL TME 75-48, December 1975.

11. J. E. Hanson, W. E. Roake, "FTR Driver Fuel Development Program Status," Proceeding of the Conference on Fast Reactor Fuel Element Technology, ANS, April 1971 p. 497.

12. Proceedings of the Conference on Fast Reactor Fuel Element Technology, ANS, 1971, Hinsdale, IL.

13. Conference on Reactor Materials Performance, Richland, Washington, Nuclear Technology 16, 1972.

14. J. W. Weber, Results of the First Interim Examination of HEDL P-23A High Cladding Temperature Subassembly, HEDL-TME 73-69, August 1973.

15. General Electric - Na Cooled Reactors, Fast Ceramic Reactor Development Program Quarterly Reports, GEAP-10028 SEries up to August 1974.

16. General Electric - Reference Fuel Studies Periodic Reports, GEAP-14032 Series, Continuing from December 1974.

17. P. S. Maiya and D. E. Busch, Journal of Nuclear Materials 44 (1972) p. 96.

18. P. S. Maiya and D. E. Busch, Met. Trans. 4 (1973) p. 663.

19. M. G. Adamson, "Reference Fuel Studies," Second Quarterly Report November 1974-January 1975, G.E. Co., GEAP-14032-2 (February 1975).

20. M. G. Adamson, "Reference Fuel Studies," Second Semi-Annual Report August 1975-January 1976, G.E. Co., GEAP-14032-4 (January 1976).

22. L. A. Lawrence and E. T. Weber, "Reirradiation of Mixed-Oxide Fuel Pins at Increased Temperatures," Transaction American Nuclear Society, Vol. 23, 1976.

23. L. A. Lawrence, R. E. Woodley, and E. T. Weber, "Cesium Relocation in Mixed-Oxide Pins Resulting from Increased Temperature Reirradiation," Transaction American Nuclear Society, Vol. 23, 1976.

24. M. G. Adamson et al, "Predictions of Fuel Cladding Chemical Interaction in Irradiated Mixed-Oxide Fuel Rods," GEAP-14075, December 1976.

25. E. A. Aitken et al, "Thermomigration and Reactions of Fission Products in Breeder Reactor Oxide Fuels 11," September 1974, (GEAP-12538).

26. P. S. Maiya and D. E. Busch, Met. Trans. 6A February 1975, p. 409.

27. E. A. Aitken et al "Transport and Reaction of Cs, Te, I, and Mo with Fast Reactor Fuel and Stainless Steel Cladding," November 1972. (GEAP-12268).

28. E. A. Aitken et al, "Thermodynamic Data Program Involving Plutonia and Urania at High Temperatures," Quarterly Report No. 17, G.E. October 1971. (GEAP-12254).

TABLE I (CONT)

NOTES FOR SUMMARY-LISTING OF IRRADIATION TESTS WITH MAJOR EMPHASIS ON FUEL CLADDING REACTION

1. LIST OF THE RANGE OF EACH VARIABLE IN THE TEST. THE PARTICULAR COMBINATION OF VARIABLES IN THE INDIVIDUAL PINS IS NOT LISTED. THIS MAY BE OBTAINED FROM THE DETAILED TEST MATRIX FOR EACH PARTICULAR TEST.

2. GETR CAPSULE TEST - 4 SMALL FUEL PINS [~101 MM(4 INCH)LONG] CONTAINING O_2 GETTERS AND Cs + T_E AS ADDITIVES.

3. PINS CONTAIN SEVERAL O_2 BUFFER/GETTER MATERIALS (Cr, Nb, V, Ti) AT DIFFERENT LOCATIONS (END PLUGS, COATED PELLETS, COATED CLADDING) WITHIN THE FUEL PIN.

4. GETR CAPSULE REIRRADIATION OF EBR-II IRRADIATED FUEL PINS (PNL-3 AND PNL-4). ADDITIONAL BURNUP IN GETR~0.6 ATOM%.

5. THERMAL FLUX HEAT RATING, EQUIVALENT TO ~29.5 W/MM (9 KW/FT) FAST FLUX.

ABBREVIATIONS USED IN TABLE

CLADDING

20% CW = 20% COLD WORK
CW = COLD WORK
A = ANNEALED
CA = CARBIDE AGGLOMERATED
20% CW-Ti = 20% COLD WORK - TITANIUM STABILIZED

FUEL

SP = SOLID PELLET
AP = ANNULAR PELLET
VP = VIPAC FUEL
RFT = RUN-TO-CLADDING BREACH

TABLE I

IRRADIATION TESTS WITH MAJOR EMPHASIS ON FUEL-CLADDING REACTION TEST VARIABLES (NOMINAL VALUES)[1]*

SITE	TEST	NO. PINS	CLADDING TYPE	MET.* CONDITION	OUTER MM DIA., (INCH)	THICKNESS MM (MILS)	FUEL TYPE*	DIA. GAP MM (MILS)	O/M	PELLET DENSITY % TD	PuO2 WT %	235U/U WT %	PEAK PIN POWER W/MM (KW/FT)	PEAK CLADDING TEMP. °C	PEAK BURNUP MWd/kg	EXPERIMENT STATUS DECEMBER 1976
ANL	08	11	316	20% CW	7.62 (0.300)	0.47 (18.5)	SP	0.18 (7)	1.97	92 91	30.0 40.0	17.27 1.5	38.7 (11.8)	700	35,55,90	1ST INTERIM EXAM - JAN, 76
GA	F-1	13	316	20% CW	7.62 (0.300)	0.47 (18.5)	AP	0.08 (3)	1.98	91	15.0 25.0		43.6 52.8 (13.3) (16.1)	680	25,50,95 120	IRRADIATION COMPLETE PIE IN PROGRESS, ALL RODS INTACT
	F-3	10	316	20% CW	7.62 (0.300)	0.47 (18.5)	SP AP	0.08 (3)	1.98 1.94	88 92	25.0		52.5 (16.0)	676 743	50,100	9 RODS BREACHED AT 50.0 MWd/kgM EXPT. TERMINATED, PIE IN PROGRESS
	F-5	46	316	20% CW (RIBBED)	7.21 7.47 (0.284) (0.294)	0.38 (15.0)	SP	0.14 (5.5)	1.96	90	25.0	28	41.0 (12.5)	720	98	DETAILED DESIGN & FABRICATION IN PROGRESS
GE	F-10	38	304 304 304 316 316 321 347	A CW CA A CW A A	6.35 (0.250)	0.38 (15.0) AND 0.25 (10.0)	SP VP	0.05 0.15 (2-6)	2.00 1.97 1.96	95 92 82	25.0	92	51.8 (15.8)	760	55,100	INTERIM, PIE AND REPORT (GEAP 14133) AT 55.0 MWd/kgM COMPLETED IRRADIATION TO 100.0 MWd/kgM TO BE COMPLETED 2/77
GE	F-11A	40	SAME AS F-10 PLUS 316	CA	6.35 (0.250)	0.38 (15)	SP VP	0.13 (5)	1.96	81 92.5	25.0	92.0	39.4 47.2 (12.0) (14.4)	620 733	55	1ST INTERIM COMPLETE (JAN.74) ON TEST STARTED RUN 79-SEPT, 75
	CAI-1[2]	4	316	20% CW	5.84 (0.230)	0.38 (15)	SP	0.14 (5.5)	1.98 1.96	90.5	25.0	65.0	44.3 (13.5)	600 750	100 HOURS MINIMUM AT TEMP. > 650°C	IRRADIATION COMPLETE PIE IN PROGRESS
	CAI-2	4	SAME AS IN CAI-1													IRRADIATION COMPLETE PIE IN PROGRESS
HEDL	P-23A	54	316	20% CW	5.84 (0.230)	0.38 (15)	SP	0.14 (5.5)	1.985 1.98 1.97	90.5	25.0	65.0	42.3 44.3 (12.9) (13.5)	698 725	11,22,45 93, RTCB(102) RBCB	INTERIMS TO 45 MWd/kg COMPLETED. PIE AT 93.00 AND ON BREACHED PIN AT 103 MWd/kgM IN REACTOR FOR RUN BEYOND CLADDING BREACH
	P-23B	59	316	20% CW	5.84 (0.230)	0.38 (15)	SP AP	0.14 (5.5)	1.97 1.95	90.5	25.0	65.0	42.6 45.0 (13.0) (13.7)	688 760	22,50,70 RTCB	INTERIMS TO 50 MWd/kg COMPLETED. IRRADIATION TO 70 MWd/kg COMPLETED. PIE IN PROGRESS. SUBASSEMBLY IN REACTOR FOR RUN TO CLADDING BREACH PROGRAM.
	P-23C	67	316	20% CW 20% CW-Ti	5.84 (0.230)	0.38 (15)	SP AP	0.14 (5.5)	1.97 1.96 1.95 1.94	90.5	25.0	65.0	41.3 43.6 (12.6) (13.3)	672 718	11,36,65 90 RTCB	INTERIMS TO 36 MWd/kgM COMPLETED. IRRADIATION TO 90 COMPLETED. PIE AT 65 AND 90 MWd/kgM IN PROGRESS. SUBASSEMBLY IN REACTOR FOR RUN TO CLADDING BREACH PROGRAM.
	P-23 SPECIAL PINS	21[3]	316	20% CW	5.84 (0.230)	0.38 (15)	SP AP	0.14 (5.5)	1.91 1.98	90.5	25.0	65.0	41.0 43.6 (12.5) (13.3)	687 736	20,35,55	12 PINS AT 20 MWd/kg OUT END RUN 80B-FEB, 76 2 PINS AT 35 MWd/kg OUT END RUN 80A-DEC, 75 7 PINS AT 55MWd/kg OUT END RUN 83-AUG,76
	RCT[4] SERIES	8	304	A	6.35 (0.250)	0.38 (15)	SP	0.14 (5.5)	1.96	94.0	25.0	0.71 45.0	36.4 (11.1)[5]	700	25,50,70	EXAMINATION COMPLETE DATA ANALYSIS IN PROGRESS

*SEE ATTACHED PAGE FOR KEY TO ABBREVIATIONS AND NOTES

TABLE II

FABRICATION AND FUEL-CLADDING CHEMICAL INTERACTION DATA FROM FUEL RODS F10B-21 AND F10B-25

	F10B-21	F10B-25
FABRICATION PARAMETERS		
FUEL COMPOSITION	UO_2-25 WT % PuO_2	UO_2-25 WT % PuO_2
FUEL O:M	1.97	2.00
CLADDING TYPE	20% CW - 316 SS	20% CW - 316 SS
FUEL SMEARED DENSITY (% TD)	91.0	91.9

	TOP OF FUEL	PEAK FLUX	TOP OF FUEL	PEAK FLUX
METALLOGRAPHIC SECTION DATA				
LOCAL BURNUP (ATOM %)	4.5	5.5	4.3	5.3
LOCAL FLUENCE, E > 0.1 MeV ($n/cm^2 \times 10^{22}$)	2.8	3.2	2.7	3.0
LOCAL LINEAR POWER w/mm (KW/FT)	39.0(11.9)	49.9(15.2)	38.0(11.6)	48.6(14.8)
LOCAL CLADDING ID TEMPERATURE °C (°F)	702(1296)	628(1162)	690(1275)	621(1150)
MAXIMUM CLADDING PENETRATION μm (IN. x10^{-3})	66(2.6)	17.8(0.7)	109(4.3)	20.3(0.8)
FRACTION OF CIRCUMFERENCE ATTACKED* (%)	40	~0	96	74

*LINEAL PERCENTAGE OF CLADDING EXHIBITING CHEMICAL ATTACK BASED ON TRANSVERSE METALLOGRAPHIC SECTIONS.

TABLE III

DESCRIPTION OF CAI-1 AND CAI-2 FUEL PINS

	PIN NO.	FUEL O:M	ADDITIVES (WT. Te, Cs & Te	BUFFER (FORM AND WT.)
CAI-1	I	1.987	Cs, Te, C (93 mg, 1:1)	Nb (PELLET O.D. COATING, ~100 mg)
	II	1.987	Cs, Te, C (93 mg, 1:1)	Nb (CENTRAL WIRE & WAFERS ~300 mg)
	III	1.987	Cs, Te, C (93 mg, 1:1)	-
	IV	1.966	Cs, Te, C (93 mg, 1:1)	-
CAI-2	V	1.989	Cs_2Te (4 mg, 2:1)	-
	VI	1.989	Cs_2Te (11 mg, 2:1)	-
	VII	1.989	Cs_2Te (11 mg, 2:1)	Nb (WASHERS, 200 mg)
	VIII	1.989	Cs_2Te (11 mg, 2:1)	Nb (PELLET COATING, 200 mg)

TABLE IV

SUMMARY OF EBR-II FUEL PINS REIRRADIATED IN GETR

		EBT-II BURNUP PRIOR TO REIRRADIATION	
		LOW BURNUP PNL-3 (2.1 at. %) PNL-4 (2.4 at. %)	MODERATE BURNUP PNL-3 (4.7 at. %) PNL-4 (6.4 at. %)
EBR-II HEAT RATING PRIOR TO REIRRADIATION	LOW POWER 17.0 - 18.8 w/mm 5.2-5.7 kw/ft	RCT-2 (PNL-3-41) SIBLING: PNL-3-26	RCT-4 (PNL-3-14) RCT-5 (PNL-3-16) SIBLING: PNL-3-15
	INTERMEDIATE POWER 27.4 - 29.4 w/mm 8.4 - 8.9 kw/ft	PCT-3 (PNL-4-61) SIBLING: PNL-4-60	RCT-1A (PNL-4-14) SIBLING: PNL-4-12

*BURNUP AND HEAT RATINGS ARE PEAK VALUES
**GETR PEAK BURNUP INCREMENT:
RCT-1A THROUGH RCT-4 0.6 ATOMS %, RCT-5 GOAL 1.2 ATOM %, ACTUAL 0.9 ATOM %
***GETR PEAK HEAT RATING: 365 W/cm (11.1 KW/FT) FOR ALL CAPSULES

THERMAL FLUX HEAT RATING YIELDING FUEL AT EQUIVALENT TO ≈29.5 W/mm (9 KW/FT) FAST FLUX HEAT RATING. PEAK HEAT RATINGS IN GETR ARE AT THE TOP OF THE FUEL COLUMN, RATHER THAN AT THE ≈ CENTER IN EBR-II, BY DESIGN.

†PNL-3 FUEL PINS: NATURAL ^{235}U ENRICHMENT
PNL-4 FUEL PINS: 45 WT % ^{235}U ENRICHMENT

TABLE V — CALCULATED VALUES FOR THE AVERAGE O/M, FUEL SURFACE O/M, AND FUEL SURFACE OXYGEN POTENTIAL FOR THE REIRRADIATED FUEL PINS AND FOR THE SIBLING FUEL PINS

FUEL PIN	LOCATION ABOVE* BOTTOM OF FUEL (mm)	AVE. O/M	FUEL SURFACE O/M	APPROX. FUEL SURFACE $-\Delta \bar{G}o_2$ (kcal / mole)
4-12	172.0	1.984	1.9998	123.5
4-14	73.7	1.986	1.9997	122.6
4-14	231.9	1.986	1.9998	102.3
3-26	169.7	1.972	1.9990	153.4
3-41	69.8	1.975	1.9995 ·	146.8
3-41	228.6	1.975	1.9995	118.8
4-60	172.2	1.969	1.9988	124.5
4-61	76.2	1.971	1.9980	129.6
4-61	234.9	1.971	1.9986	108.8
3-15	170.2	1.986	1.9991	125.6
3-14	44.5	1.990	1.9996	116.9
3-14	256.5	1.990	1.9998	96.0

* TOTAL LENGTH OF FUEL COLUMN IS 340.4 mm

TABLE VII — MEASUREMENTS OF CLADDING PENETRATION FROM FCCI ON HEDL P-23A FUEL PINS

PIN	FUEL BURNUP - AT. % AVG.	PEAK	CLADDING TEMPERATURE-°C	DEPTH OF ATTACK - μm AVG.	MAX.
P-23A-58B	1.0	1.2	440	0	0
			520	1.3	1.3
			588	3.2	6.4
			670	7.2	13.2
			718	13.5	38.1
P-23A-26	2.1	2.4	440	0	0
			520	1.3	1.3
			588	3.3	7.6
			670	9.0	12.7
			718	18.4	38.1
P-23A-25	4.6	5.0	421	0	0
			512	0	1.3
			590	9.4	17.8
			668	16.6	30.5
			700	21.9	33.0
			715	26.9	50.8

TABLE VI — MAXIMUM EXTENT OF FUEL-CLADDING CHEMICAL INTERACTION

CAPSULE (PIN)	INITIAL ^{235}U/U	BURNUP* ATOM%	MAXIMUM REACTION DEPTH μm (mils)	CLADDING INNER SURFACE TEMPERATURE	CHARACTER
RCT-1A (PNL-4-14)	45%	7.0	40.6 (1.6)	670°C	INTERGRANULAR**
RCT-2 (PNL-3-41)	0.71%	2.8	12.7 (0.5)	650°C	COMBINED
RCT-3 (PNL-4-61)	45%	3.0	12.7 (0.5)	700°C	COMBINED
RCT-4 (PNL-3-14)	0.71%	5.3	61.0 (2.4)	700°C	COMBINED (LOCALIZED)

* COMBINED EBR-II + GETR (GETR CONTRIBUTION~0.65 ATOM%)

** SIMILAR TO REACTIONS SEEN IN P-23A FUEL PINS AT 1.1 ATOM% BURNUP (1100 HOURS)

TABLE VIII — COMPARISON OF MEASURED AND CALCULATED CLADDING PENETRATIONS

CLADDING SURFACE TEMPERATURE °C	°F	MEASURED PENETRATION ON P-23A PIN AVG. μm (mil)	MAX μm (mil)	CALCULATED PENETRATION USING CORRELATIONS AVG. HEDL μm (mil)	MAX GE μm (mil)
590	1095	9.4 (0.37)	17.8 (0.7)	6.4 (0.25)	33.0 (1.03)
668	1235	16.5 (0.65)	30.5 (1.2)	16.5 (0.65)	51.8 (2.04)
701	1295	21.8 (0.86)	33.0 (1.3)	23.6 (0.93)	67.3 (2.65)
715	1320	26.9 (1.06)	50.8 (2.0)	27.2 (1.07)	74.7 (2.94)

Burnup at% - PEAK 5.3, AVG. 4.9
O/M - 1.984
TIME OF IRRADIATION - 192.2 DAYS
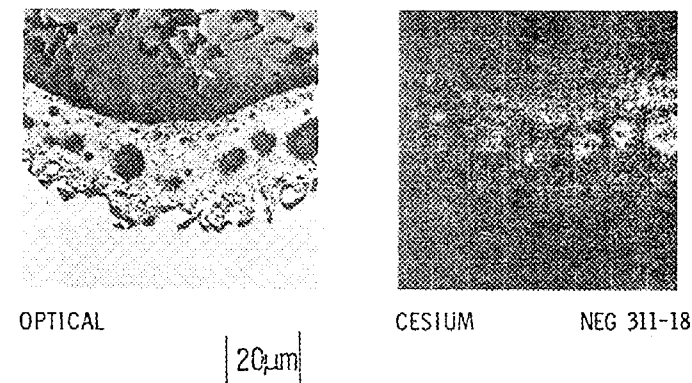PEAK PIN POWER 43.0 w/mm (13.1 kW/FT)
SMEAR DENSITY - 86.1% TD.

FIGURE 1. TYPICAL MATRIX CLADDING ATTACK AT 1.2 AT % BURNUP FOR CLADDING TEMPERATURE FROM 575°C TO 675°C. 316-20% CW STAINLESS STEEL O/M 1.98.
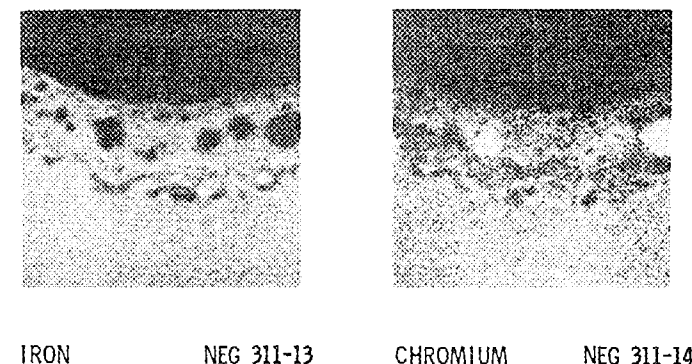

FIGURE 2. TYPICAL INTERGRANULAR CLADDING ATTACK AT 1.2 AT % BURNUP FOR CLADDING TEMPERATURES AT 690°C. 316-20% CW STAINLESS STEEL. O/M 1.98.

OPTICAL   CESIUM   NEG 311-18

IRON   NEG 311-13   CHROMIUM   NEG 311-14

FIGURE 3. CLADDING AND FISSION PRODUCT DISTRIBUTION MATRIX ATTACK OF 316-20% CW STAINLESS STEEL AT A TEMPERATURE OF 670°C. BURNUP 2.4 AT % O/M 1.98.
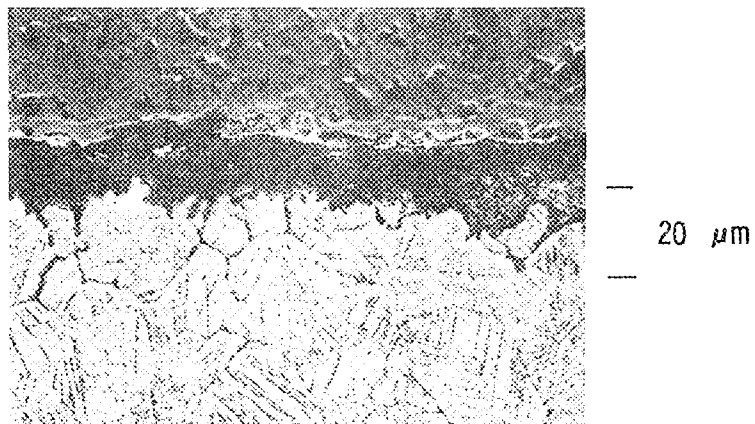
FIGURE 4. INTERGRANULAR CLADDING ATTACK AT 2.4 AT % FOR CLADDING
TEMPERATURE 675°C 316-20% CW STAINLESS, O/M-1.98.

FIGURE 6. MATRIX CLADDING ATTACK ON FUEL PIN P-23B-62D. FUEL
FUEL O/M 1.95 BURNUP 2.3 AT % CLADDING TEMPERATURE 690°C.
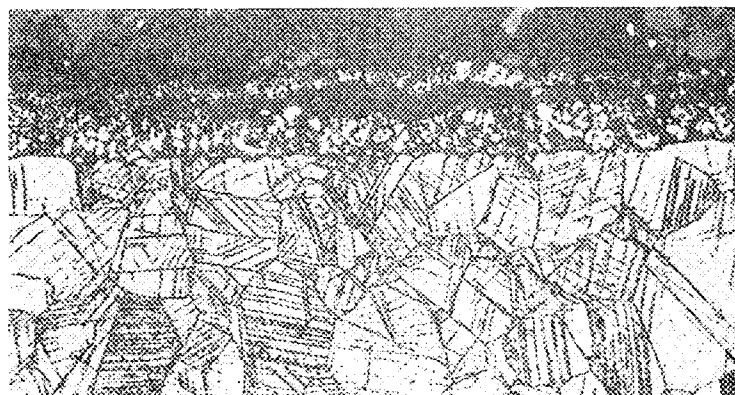
FIGURE 5. MATRIX CLADDING ATTACK ON FUEL PIN P-23B-49C. FUEL
O/M 1.97 BURNUP 2.3 AT %. CLADDING TEMPERATURE 690°C.
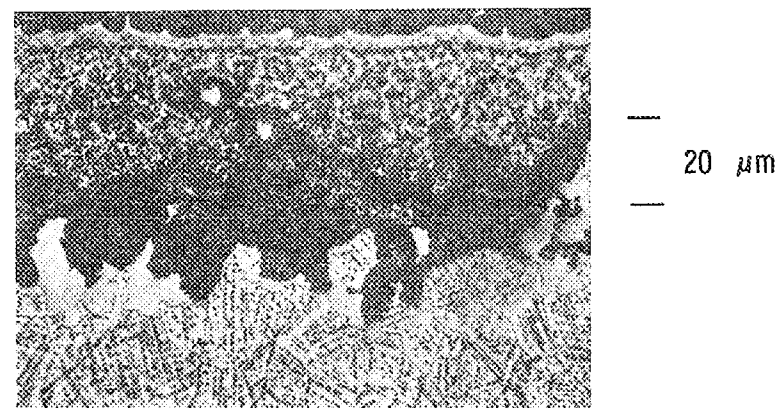
FIGURE 7. EVOLVED MATRIX CLADDING ATTACK. FUEL BURNUP 5.0 AT % CLADDING
TEMPERATURE >675°C. FUEL O/M 1.98.

OPTICAL   IRON   CHROMIUM
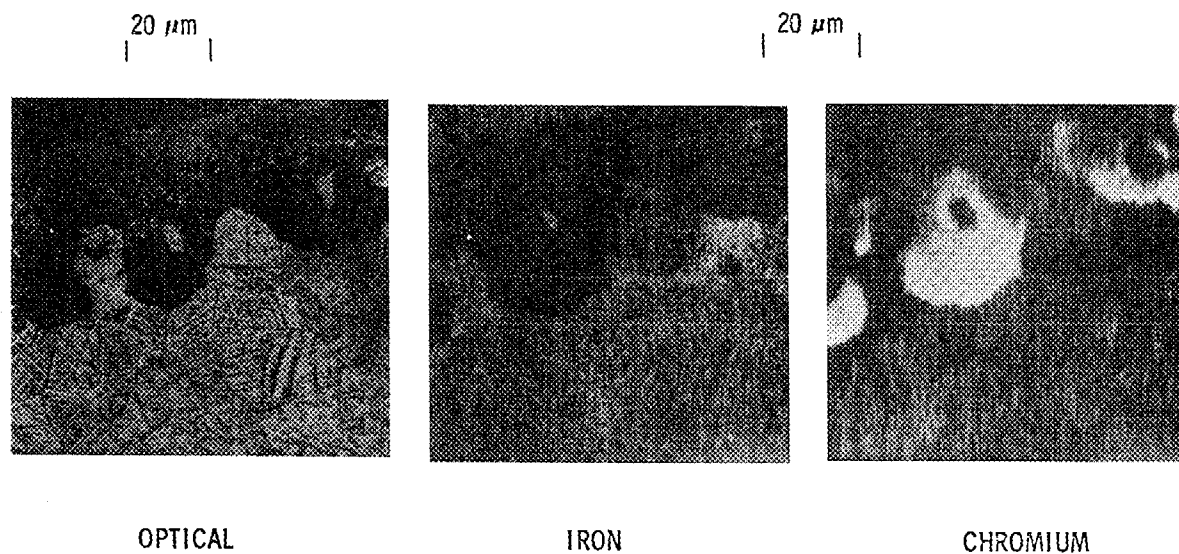
FIGURE 8. ELECTRON MICROPROBE EXAMINATION SHOWING Fe AND Cr DISTRIBU-
TION IN GRAINS & GRAIN BOUNDARIES OF EVOLVED MATRIX CLADDING
ATTACK. FUEL B.U. 5.3 AT % CLADDING TEMPERATURE $>680^{\circ}$C. O/M
1.98.

CLADDING   FUEL   IRON   NICKEL
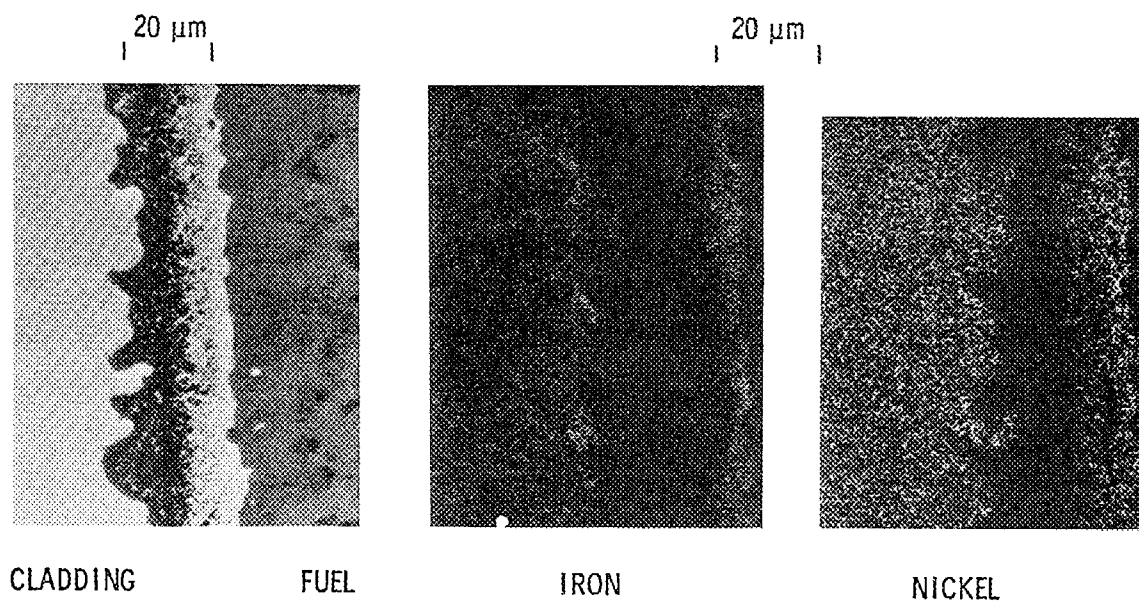
FIGURE 9. ELECTRON MICROPROBE. EXAMINATION SHOWING Fe AND Ni IN
CLADDING WITH EVOLVED MATRIX ATTACK FUEL B.U. 5.3 AT %
O/M 1.98 CLADDING TEMPERATURE $\sim 680^{\circ}$C.

|20 μm|

CLADDING   FUEL

20 μm

FIGURE 11.   MATRIX REACTION ON CLADDING OF FUEL PIN P-23B-2A
FUEL BURNUP 5.3 AT %, O/M-1.97 TEMPERATURE >675°C.

CHROMIUM   CESIUM

FIGURE 10. CHROMIUM AND CESIUM DISTRIBUTION IN SAME AREA OF CLADDING
FUEL GAP AS IN FIGURE 9.
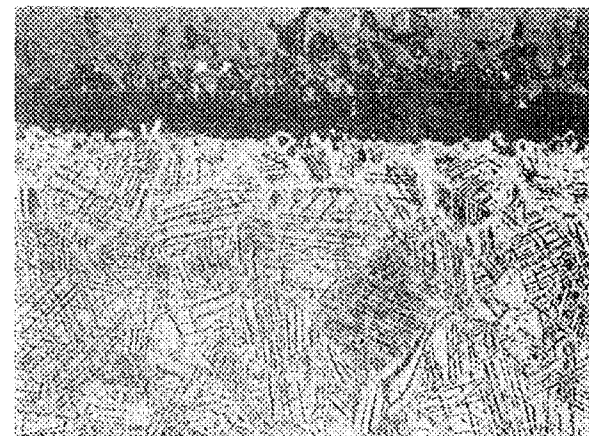
FIGURE 12.   MATRIX REACTION ON P-23B-40B IS LESS THAN ON 23B-2A
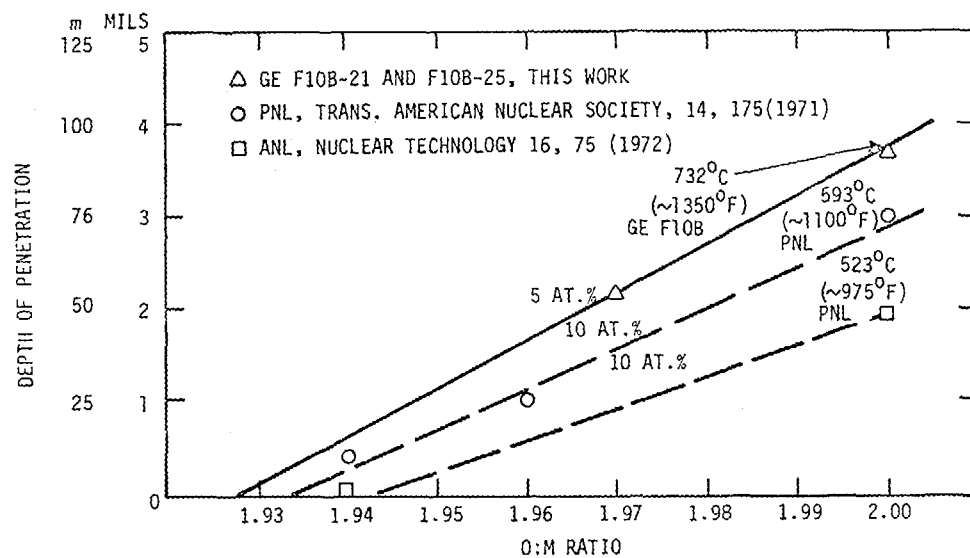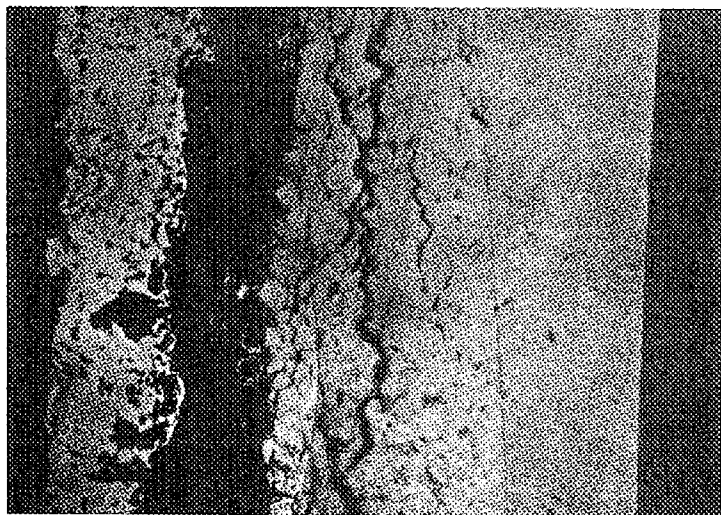FIGURE 11. FUEL O/M 1.95 IS LESS THAN IN P-23B-2A.
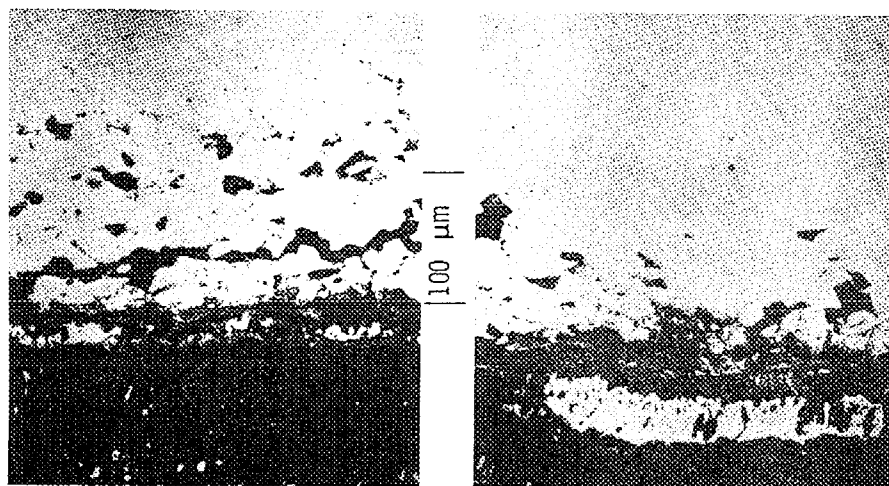TEMPERATURE AND B.U. ARE EQUAL.

FIGURE 13. DEPTH OF CLADDING PENETRATION VS INITIAL FUEL O/M AT 523°C, 593°C AND 732°C.

FIGURE 14. PHOTOMACROGRAPH OF LONGITUDINAL SECTION FROM FUEL ROD 1 OF CAI-1 SHOWING EROSION OF CLADDING.

100 µm

(A) CAI-1 FUEL ROD IV

(B) CAI-1 FUEL ROD II

100 µm

FIGURE 15. PHOTOMICROGRAPHS OF SELECTED REGIONS OF CLADDING FROM CAI-1 FUEL RODS IV AND I.
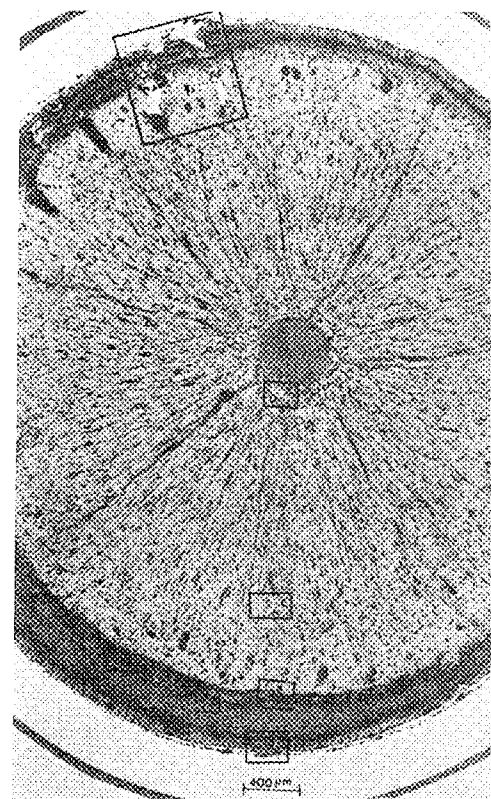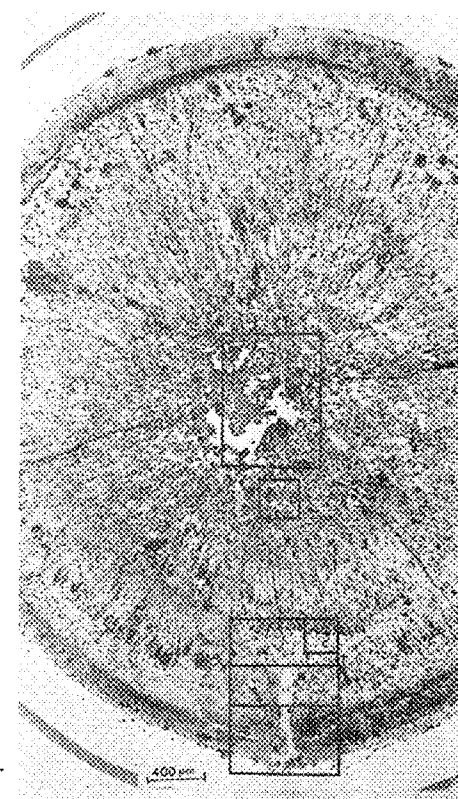
A
CAI-1-I

B
CAI-1-II

FIGURE 16. PHOTOMOSAICS OF TRANSVERSE SECTIONS FROM CAI-1 FUEL PINS I(a) AND II b.
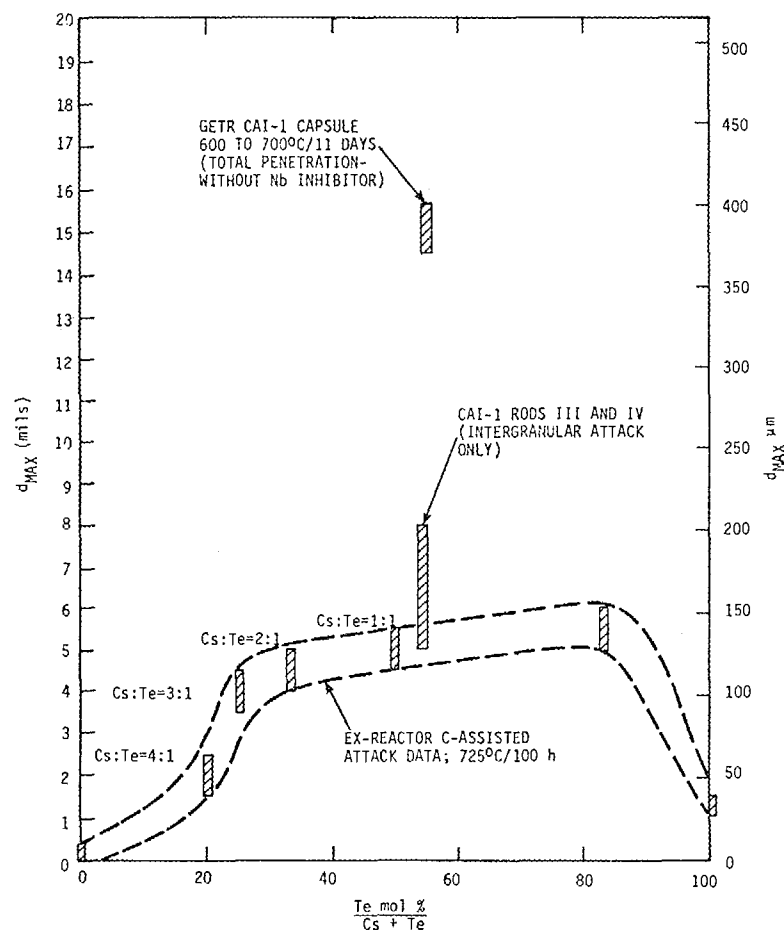
FIGURE 17. COMPARISON OF IN-REACTOR AND EX-REACTOR Cs, Te-INDUCED ATTACK RESULTS FOR TYPE 316 STAINLESS STEEL CLADDING.

Key labels in Figure 17: GETR CAI-1 CAPSULE 600 TO 700°C/11 DAYS (TOTAL PENETRATION-WITHOUT Nb INHIBITOR); CAI-1 RODS III AND IV (INTERGRANULAR ATTACK ONLY); Cs:Te=1:1; Cs:Te=2:1; Cs:Te=3:1; Cs:Te=4:1; EX-REACTOR C-ASSISTED ATTACK DATA; 725°C/100 h.

Axes: d_{MAX} (mils); d_{MAX} μm; $\dfrac{Te\ mol\ \%}{Cs + Te}$

FUEL

25 w/o PuO_2-75 w/o UO_2

O/M 1.985 ⟶ 1.97
MECHANICALLY MIXED
SOLID PELLET
 90.4% TD
 DISHED ENDS
 5.3mm LONG x 4.9mm DIAM.
34.3cm LONG FUEL COLUMN
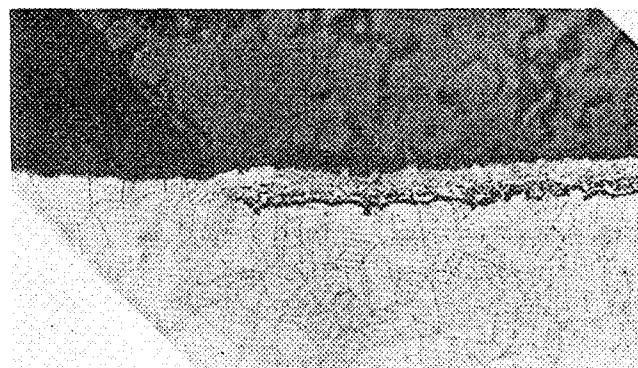FUEL PIN SMEARED DENSITY 85.5% TD

CLADDING

 316SS-20% COLD WORKED
 5.84mm OD x 0.38mm THICK WALL

OPERATING CONDITIONS

 LINEAR POWER - 39.4mm
 CLADDING INSIDE SURFACE - 410°C to 720°C
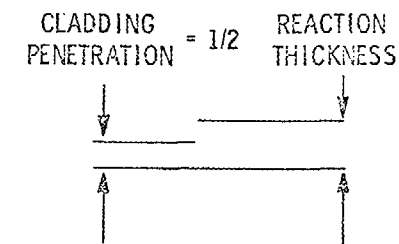 PEAK EXPOSURES - 1.2, 2.4, 5.0 AT. % BURNUP

FIGURE 18. DESCRIPTION OF P-23A FUEL PINS IRRADIATED IN EBR-II.

FIGURE 19. PHOTOMICROGRAPH SHOWING CRITERIA FOR MEASURING DEPTH OF MATRIX ATTACK ON CLADDING.

Labels: FUEL; FUEL CRACK; CLADDING; CLADDING PENETRATION = 1/2 REACTION THICKNESS.

MEASURED	PREDICTED	AVG. BURNUP AT.%
□	——	1.0
△	——	2.1
○	——	4.6

Axes: DEPTH OF PENETRATION (MICRONS / MILS); TEMPERATURE OF CLADDING INSIDE SURFACE, °C/°F
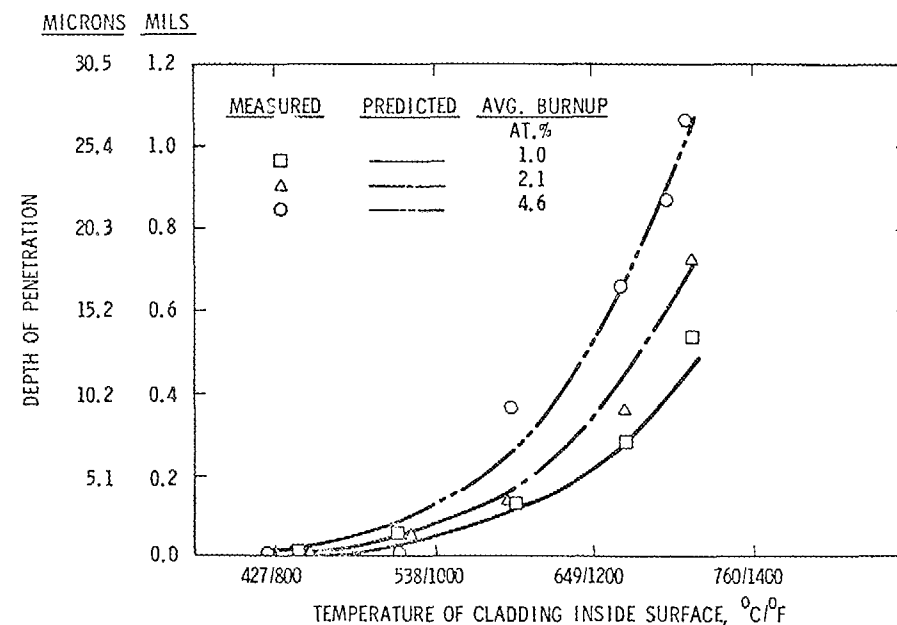
FIGURE 20. MEASURED DEPTH OF CLADDING ATTACK ON P-23A PINS AND PREDICTED DEPTH OF CLADDING ATTACK USING HEDL CORRELATION

$$D = 1.107 \times 10^6 \text{EXP}\left[\frac{-14185}{1.98\ T(^\circ K)}\right] t(0:M + 0.001\ B.U. - 1.96)Q^{2.33}(1-P)$$

(1) $T_{CLAD} = 704^\circ C\ (1300^\circ F)$
  $P = 0.85\ \%\ TD$
  $Q = 49.2\ W/MM\ (15\ KW/FT)$
  $0:M = 1.96$
  $B.U.\ 16.7\ AT.\ \%$

(2) $T_{CLAD} = 538^\circ C\ (1000^\circ F)$
  $P = 0.85\ \%\ TD$
  $Q = 28.9\ W/MM\ (8.8\ KW/FT)$
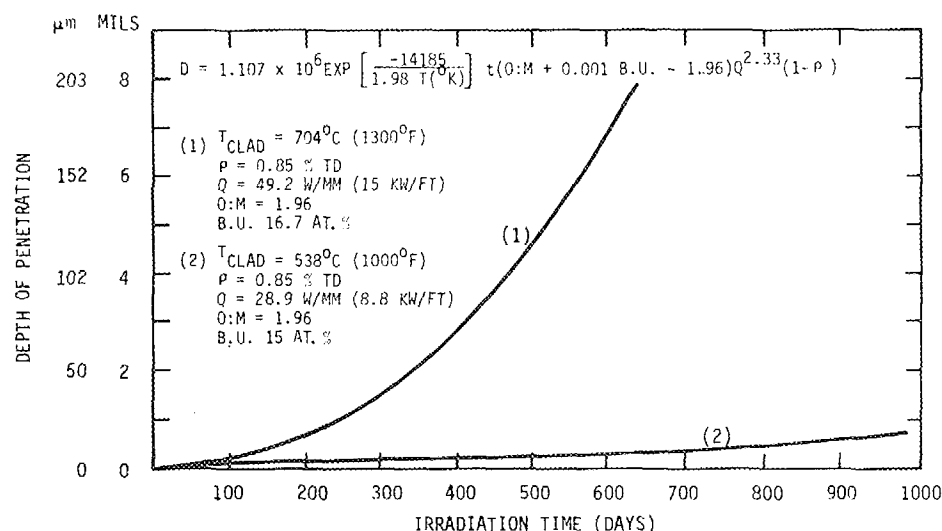 $0:M = 1.96$
  $B.U.\ 15\ AT.\ \%$

FIGURE 21. PREDICTED DEPTH OF CLADDING ATTACK FOR TWO SETS OF OPERATING CONDITIONS USING G.E. CORRELATION.
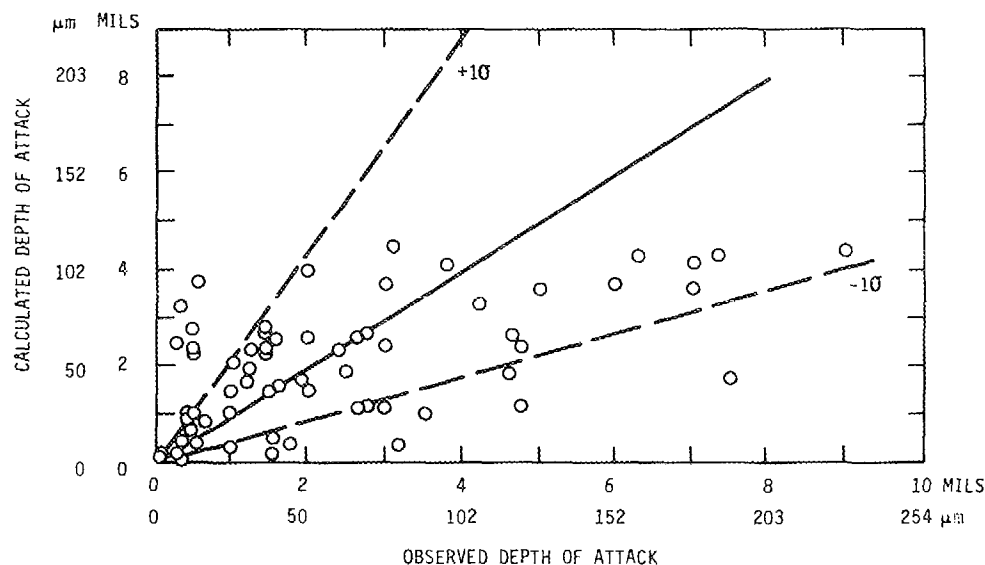
FIGURE 22. MEASURED VS PREDICTED DEPTH OF CLADDING ATTACK USING G.E. CORRELATION.

Fuel-Cladding Mechanical Interaction Effects in Fast Reactor Mixed Oxide Fuel, by A. Boltax, A. Biancheria, the United States.

ABSTRACT

Thermal and fast reactor irradiation experiments on mixed oxide fuel pins under steady-state and power change conditions reveal evidence for significant fuel-cladding mechanical interaction (FCMI) effects. Analytical studies with the LIFE-III fuel performance code indicate that high cladding stresses can be produced by general and local FCMI effects. Also, evidence is presented to show that local cladding strains can be caused by the accumulation of cesium at the fuel-cladding interface. Although it is apparent that steady-state FCMI effects have not given rise to cladding breaches in current fast reactors, it is anticipated that FCMI may become more important in the future because of interest in: higher fuel burnups; increased power ramp rates; load follow operation; and low swelling cladding alloys.

I. INTRODUCTION

A basic objective of fast reactor irradiation studies of mixed oxide fuel pins is to systematically determine performance limits as functions of design and operating parameters. This paper focuses attention on one aspect of fuel pin irradiation behavior, namely, fuel cladding mechanical interaction, and examines its significance with respect to overall fuel behavior.

The core materials for the world's first generation of prototype LMFBR's will consist of mixed oxide fuel and stainless steel cladding and structural materials. The successful high burnup irradiation behavior (>12% burnup) of mixed oxide pins with stainless steel cladding has been demonstrated by the French in Rapsodie, the UK in DFR, the Russians in BOR-60, and the US in EBR-II, as well as others. This successful development program, covering the period 1965 to the present, has generated substantial information about the physical phenomena which must be considered in fuel pin design. Although we can point with pride at these achievements, it is clear that the future requirements of commercial-high breeding gain LMFBR's will place greater demands on fuel performance.